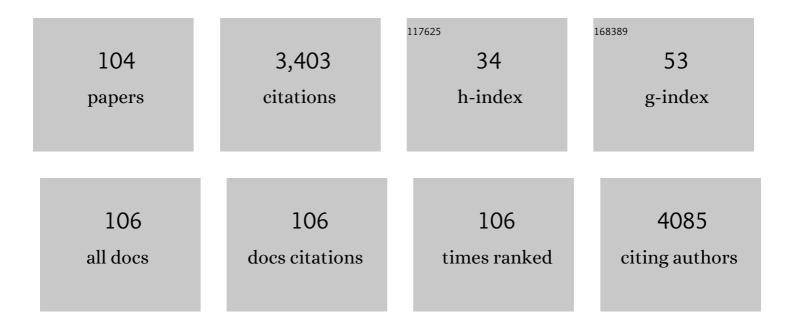
List of Publications by Year in descending order

Source: https://exaly.com/author-pdf/2133363/publications.pdf Version: 2024-02-01



#	Article	IF	CITATIONS
1	Efficient degradation of tetracycline by singlet oxygen-dominated peroxymonosulfate activation with magnetic nitrogen-doped porous carbon. Journal of Environmental Sciences, 2022, 115, 330-340.	6.1	85
2	Asymmetric Hybrid Siloxane Side Chains for Enhanced Mobility and Mechanical Properties of Diketopyrrolopyrroleâ€Based Polymers. Macromolecular Rapid Communications, 2022, 43, e2100636.	3.9	6
3	Electrically controllable reflection bandwidth polymer-stabilized cholesteric liquid crystals with low operating voltage. Liquid Crystals, 2022, 49, 1314-1321.	2.2	5
4	Deep Ultraviolet Light Stimulated Synaptic Transistors Based on Poly(3-hexylthiophene) Ultrathin Films. ACS Applied Materials & Interfaces, 2022, 14, 11718-11726.	8.0	19
5	Purification and characterization of anti-phytopathogenic fungi angucyclinone from soil-derived Streptomyces cellulosae. Folia Microbiologica, 2022, 67, 517-522.	2.3	4
6	Side Chain Engineering: Achieving Stretch-Induced Molecular Orientation and Enhanced Mobility in Polymer Semiconductors. Chemistry of Materials, 2022, 34, 2696-2707.	6.7	17
7	Role of Molecular Weight in the Mechanical Properties and Charge Transport of Conjugated Polymers Containing Siloxane Side Chains. Macromolecular Rapid Communications, 2022, , 2200149.	3.9	4
8	Tuning of polymer-wall surface components and its effect on the optoelectronic performance of liquid crystal devices with polymer walls. Molecular Crystals and Liquid Crystals, 2022, 736, 93-102.	0.9	1
9	Band-edge-enhanced tunable random laser using a polymer-stabilised cholesteric liquid crystal. Liquid Crystals, 2021, 48, 255-262.	2.2	11
10	Enhanced Strategies for Antibiotic Removal from Swine Wastewater in Anaerobic Digestion. Trends in Biotechnology, 2021, 39, 8-11.	9.3	51
11	Deep Blue Layered Lead Perovskite Lightâ€Emitting Diode. Advanced Optical Materials, 2021, 9, 2001709.	7.3	20
12	Physical properties of liquid crystals doped with CsPbBr ₃ quantum dots. Liquid Crystals, 2021, 48, 1357-1364.	2.2	7
13	Tri-state switching of a high-order parameter, double-layered guest-host liquid-crystal shutter, doped with the mesogenic molecule 4HPB. Liquid Crystals, 2021, 48, 1555-1561.	2.2	9
14	Synthesis of 0D Manganeseâ€Based Organic–Inorganic Hybrid Perovskite and Its Application in Leadâ€Free Red Lightâ€Emitting Diode. Advanced Functional Materials, 2021, 31, 2100855.	14.9	98
15	Light-Emitting Diodes with Manganese Halide Tetrahedron Embedded in Anti-Perovskites. ACS Energy Letters, 2021, 6, 1901-1911.	17.4	17
16	Liquid Crystal Polarisation Converter Arrays Based on Microholes Patterned Hydrophobic Layers. Liquid Crystals, 2021, 48, 1873-1879.	2.2	3
17	Taming Charge Transport and Mechanical Properties of Conjugated Polymers with Linear Siloxane Side Chains. Macromolecules, 2021, 54, 5440-5450.	4.8	18
18	Ultrathin Polythiophene Films Prepared by Vertical Phase Separation for Highly Stretchable Organic Field‣ffect Transistors, Advanced Electronic Materials, 2021, 7, 2100591.	5.1	11

#	Article	IF	CITATIONS
19	Circularly Polarized Photodetectors Based on Chiral Materials: A Review. Frontiers in Chemistry, 2021, 9, 711488.	3.6	42
20	Intrinsically Stretchable <i>n</i> -Type Polymer Semiconductors through Side Chain Engineering. Macromolecules, 2021, 54, 8849-8859.	4.8	27
21	Solutionâ€Processed Ultrathin Semiconductor Films for Highâ€Performance Ammonia Sensors. Advanced Materials Interfaces, 2021, 8, 2100493.	3.7	4
22	Electrically controlled switching of mixed mode laser within the band-gap of cholesteric liquid crystals, 2021, 48, 1268-1275.	2.2	2
23	Sequential vertical flow trickling filter and horizontal flow multi-soil-layering reactor for treatment of decentralized domestic wastewater with sodium dodecyl benzene sulfonate. Bioresource Technology, 2020, 300, 122634.	9.6	31
24	Photocatalytic performances of heterojunction catalysts of silver phosphate modified by PANI and Cr-doped SrTiO3 for organic pollutant removal from high salinity wastewater. Journal of Colloid and Interface Science, 2020, 561, 379-395.	9.4	27
25	Insights into mechanisms of UV/ferrate oxidation for degradation of phenolic pollutants: Role of superoxide radicals. Chemosphere, 2020, 244, 125490.	8.2	88
26	Microalgal and duckweed based constructed wetlands for swine wastewater treatment: A review. Bioresource Technology, 2020, 318, 123858.	9.6	74
27	Construction of Builtâ€In Electric Field within Silver Phosphate Photocatalyst for Enhanced Removal of Recalcitrant Organic Pollutants. Advanced Functional Materials, 2020, 30, 2002918.	14.9	133
28	Azaisoindigo-Based Polymers with a Linear Hybrid Siloxane-Based Side Chain for High-Performance Semiconductors Processable with Nonchlorinated Solvents. ACS Applied Materials & Interfaces, 2020, 12, 41832-41841.	8.0	14
29	Enabling discrimination capability in an achiral F6BT-based organic semiconductor transistor <i>via</i> circularly polarized light induction. Journal of Materials Chemistry C, 2020, 8, 9271-9275.	5.5	22
30	Induction of circularly polarized electroluminescence from achiral poly(fluorene- <i>alt</i> -benzothiadiazole) by circularly polarized light. Journal of Materials Chemistry C, 2020, 8, 6521-6527.	5.5	20
31	Air-Stable and High-Performance Unipolar n-Type Conjugated Semiconducting Polymers Prepared by a "Strong Acceptor–Weak Donor―Strategy. ACS Applied Materials & Interfaces, 2020, 12, 17790-1779	8 ^{8.0}	18
32	Sustainable livestock wastewater treatment via phytoremediation: Current status and future perspectives. Bioresource Technology, 2020, 315, 123809.	9.6	104
33	Preparation, Performances, and Mechanisms of Microbial Flocculants for Wastewater Treatment. International Journal of Environmental Research and Public Health, 2020, 17, 1360.	2.6	44
34	Polymer-stabilised cholesteric liquid-crystals as tunable light-reflector with low operating-voltage and energy consumption. Liquid Crystals, 2020, 47, 1655-1662.	2.2	9
35	Performance and Biomass Characteristics of SBRs Treating High-Salinity Wastewater at Presence of Anionic Surfactants. International Journal of Environmental Research and Public Health, 2020, 17, 2689.	2.6	4
36	Effect of presence of hydrophilic volatile organic compounds on removal of hydrophobic n-hexane in biotrickling filters. Chemosphere, 2020, 252, 126490.	8.2	42

#	Article	IF	CITATIONS
37	Highly polarized absorption and emission from polymer-stabilized smectic guest-host systems. Liquid Crystals, 2019, 46, 1574-1583.	2.2	6
38	Enhanced activation of peroxymonosulfte by LaFeO3 perovskite supported on Al2O3 for degradation of organic pollutants. Chemosphere, 2019, 237, 124478.	8.2	72
39	Enhanced mid infrared emission of erbium doped fluoro-zinc glass-ceramics. Materials Research Express, 2019, 6, 115206.	1.6	2
40	Rational molecular design for isoindigo-based polymer semiconductors with high ductility and high electrical performance. Journal of Materials Chemistry C, 2019, 7, 11639-11649.	5.5	16
41	Modulating charge transport characteristics of bis-azaisoindigo-based D–A conjugated polymers through energy level regulation and side chain optimization. Journal of Materials Chemistry C, 2019, 7, 7618-7626.	5.5	23
42	High-efficiency synthesis of a naphthalene-diimide-based conjugated polymer using continuous flow technology for organic field-effect transistors. Journal of Materials Chemistry C, 2019, 7, 8450-8456.	5.5	12
43	Side-Chain Engineering To Optimize the Charge Transport Properties of Isoindigo-Based Random Terpolymers for High-Performance Organic Field-Effect Transistors. Macromolecules, 2019, 52, 4765-4775.	4.8	23
44	Aza-Based Donor-Acceptor Conjugated Polymer Nanoparticles for Near-Infrared Modulated Photothermal Conversion. Frontiers in Chemistry, 2019, 7, 359.	3.6	7
45	Tuning helical twisting power and photoisomerisation kinetics of axially chiral cyclic azobenzene dopants in cholesteric liquid crystals. Liquid Crystals, 2019, 46, 2181-2189.	2.2	15
46	Effects of copper ions on removal of nutrients from swine wastewater and on release of dissolved organic matter in duckweed systems. Water Research, 2019, 158, 171-181.	11.3	108
47	Highly Sensitive Polymer Phototransistor Based on the Synergistic Effect of Chemical and Physical Blending in D (Donor)–A (Acceptor) Copolymers. Advanced Electronic Materials, 2019, 5, 1900174.	5.1	12
48	Fused Heptacyclic-Based Acceptor–Donor–Acceptor Small Molecules: N-Substitution toward High-Performance Solution-Processable Field-Effect Transistors. Chemistry of Materials, 2019, 31, 2027-2035.	6.7	33
49	Fast and deep oxidative desulfurization of dibenzothiophene with catalysts of MoO ₃ –TiO ₂ @MCM-22 featuring adjustable Lewis and BrÃ,nsted acid sites. Catalysis Science and Technology, 2019, 9, 6166-6179.	4.1	43
50	Sb ₂ S ₃ solar cells: functional layer preparation and device performance. Inorganic Chemistry Frontiers, 2019, 6, 3381-3397.	6.0	33
51	Adsorptive removal of anionic dye using calcined oyster shells: isotherms, kinetics, and thermodynamics. Environmental Science and Pollution Research, 2019, 26, 5944-5954.	5.3	62
52	Chirality detection of amino acid enantiomers by organic electrochemical transistor. Biosensors and Bioelectronics, 2018, 105, 121-128.	10.1	73
53	Responses of microalgae Coelastrella sp. to stress of cupric ions in treatment of anaerobically digested swine wastewater. Bioresource Technology, 2018, 251, 274-279.	9.6	114
54	Improved Transistor Performance of Isoindigo-Based Conjugated Polymers by Chemically Blending Strongly Electron-Deficient Units with Low Content To Optimize Crystal Structure. Macromolecules, 2018, 51, 370-378.	4.8	36

#	Article	IF	CITATIONS
55	High-contrast electrically switchable light-emitting liquid crystal displays based on α-cyanostilbenic derivative. Liquid Crystals, 2018, 45, 32-39.	2.2	12
56	Highly selective and sensitive sensor based on an organic electrochemical transistor for the detection of ascorbic acid. Biosensors and Bioelectronics, 2018, 100, 235-241.	10.1	103
57	Performance and biofilm characteristics of biotrickling filters for ethylbenzene removal in the presence of saponins. Environmental Science and Pollution Research, 2018, 25, 30021-30030.	5.3	42

#	Article	IF	CITATIONS
73	Nanofiber-structured hydrogel yarns with pH-response capacity and cardiomyocyte-drivability for bio-microactuator application. Acta Biomaterialia, 2017, 60, 144-153.	8.3	16
74	Characterisation and effect of polymer network deformation in reverse-mode polymer-stabilised cholesteric texture. Liquid Crystals, 2017, 44, 437-443.	2.2	11
75	Regulation and control of polymer network deformation in reverse-mode polymer-stabilised cholesteric texture. Liquid Crystals, 2017, 44, 688-694.	2.2	8
76	A Fast Response Ammonia Sensor Based on Coaxial PPy–PAN Nanofiber Yarn. Nanomaterials, 2016, 6, 121.	4.1	32
77	Continuously tunable emission color based on the molecular aggregation of (2Z,2′Z)-2,2′-(1,4-phenylenae)bis(3-(4-(dodecyloxy)phenyl)acrylonitrile). RSC Advances, 2016, 6, 96196-962	20 ³ 16	6
78	Solutionâ€Processed Microporous Semiconductor Films for Highâ€Performance Chemical Sensors. Advanced Materials Interfaces, 2016, 3, 1600518.	3.7	47
79	Bis(2-oxoindolin-3-ylidene)-benzodifuran-dione and bithiophene-based conjugated polymers for high performance ambipolar organic thin-film transistors: the impact of substitution positions on bithiophene units. Journal of Materials Chemistry C, 2016, 4, 6391-6400.	5.5	15
80	Fabrication of Aligned Nanofiber Polymer Yarn Networks for Anisotropic Soft Tissue Scaffolds. ACS Applied Materials & Interfaces, 2016, 8, 16950-16960.	8.0	102
81	Enhanced near-infrared photoresponse of organic phototransistors based on single-component donor–acceptor conjugated polymer nanowires. Nanoscale, 2016, 8, 7738-7748.	5.6	65
82	The effect of MWS polarisation on the morphology and electro-optical behaviour of normal-mode polymer-stabilised cholesteric textures. Liquid Crystals, 2016, 43, 540-546.	2.2	2
83	An ABA triblock copolymer strategy for intrinsically stretchable semiconductors. Journal of Materials Chemistry C, 2015, 3, 3599-3606.	5.5	93
84	Cell gap effects on domain size and electro-optical properties of normal-mode polymer-stabilised cholesteric texture. Liquid Crystals, 2015, 42, 255-260.	2.2	8
85	A new thieno-isoindigo derivative-based D–A polymer with very low bandgap for high-performance ambipolar organic thin-film transistors. Polymer Chemistry, 2015, 6, 3970-3978.	3.9	36
86	High-efficiency self-healing conductive composites from HPAMAM and CNTs. Journal of Materials Chemistry A, 2015, 3, 12154-12158.	10.3	21
87	Bis(2-oxoindolin-3-ylidene)-benzodifuran-dione-based D–A polymers for high-performance n-channel transistors. Polymer Chemistry, 2015, 6, 2531-2540.	3.9	32
88	Cholesteric liquid crystals with an electrically controllable reflection bandwidth based on ionic polymer networks and chiral ions. Journal of Materials Chemistry C, 2015, 3, 5406-5411.	5.5	18
89	Au-Induced Directional Growth of Inkjet-Printed 6,13-Bis(triisopropylsilylethynyl) Pentacene. Journal of Display Technology, 2015, 11, 450-455.	1.2	4
90	Phototransistors based on a donor–acceptor conjugated polymer with a high response speed. Journal of Materials Chemistry C, 2015, 3, 10734-10741.	5.5	26

#	Article	IF	CITATIONS
91	A phthalimide- and diketopyrrolopyrrole-based A ₁ –ï€â€"A ₂ conjugated polymer for high-performance organic thin-film transistors. Polymer Chemistry, 2015, 6, 418-425.	3.9	15
92	Thickness dependence of the electro-optical properties of reverse-mode polymer-stabilised cholesteric texture. Liquid Crystals, 2014, 41, 1382-1387.	2.2	16
93	Inkjet Printed Poly(3-hexylthiophene) Thin-Film Transistors: Effect of Self-Assembled Monolayer. Molecular Crystals and Liquid Crystals, 2014, 593, 201-213.	0.9	2
94	Influence of Curing Frequency on the Morphology and the Electro-Optical Property of Polymer-Stabilized Cholesteric Textures. Molecular Crystals and Liquid Crystals, 2014, 588, 9-16.	0.9	3
95	Submillisecond-Response Light Shutter for Solid-State Volumetric 3D Display Based on Polymer-Stabilized Cholesteric Texture. Journal of Display Technology, 2014, 10, 396-401.	1.2	10
96	A bis(2-oxoindolin-3-ylidene)-benzodifuran-dione containing copolymer for high-mobility ambipolar transistors. Chemical Communications, 2014, 50, 3180.	4.1	72
97	Electrically switchable photoluminescence of fluorescent-molecule-dispersed liquid crystals prepared via photoisomerization-induced phase separation. Journal of Materials Chemistry C, 2014, 2, 1386.	5.5	52
98	A luminescent liquid crystal with multistimuli tunable emission colors based on different molecular packing structures. New Journal of Chemistry, 2014, 38, 3429.	2.8	44
99	Self-stratified semiconductor/dielectric polymer blends: vertical phase separation for facile fabrication of organic transistors. Journal of Materials Chemistry C, 2013, 1, 3989.	5.5	59
100	Benzotrithiophene and benzodithiophene-based polymers for efficient polymer solar cells with high open-circuit voltage. Polymer Chemistry, 2013, 4, 3390.	3.9	15
101	Low-temperature melt processed polymer blend for organic thin-film transistors. Journal of Materials Chemistry, 2012, 22, 18887.	6.7	17
102	Polymer blends with semiconducting nanowires for organic electronics. Journal of Materials Chemistry, 2012, 22, 4244.	6.7	66
103	Organic thin-film transistors with a photo-patternable semiconducting polymer blend. Journal of Materials Chemistry, 2011, 21, 15637.	6.7	29
104	Tensile properties of two-dimensional poly(3-hexyl thiophene) thin films as a function of thickness. Journal of Materials Chemistry C, 0, , .	5.5	1